



On the Fiber Texture Change during Drawing of initial{112}<111>and Goss Orientations in Aluminum Rod

メタデータ	言語: eng 出版者: 公開日: 2010-04-06 キーワード (Ja): キーワード (En): 作成者: Inakazu, Naotsugu, Yamamoto, Hisashi, Inoue, Hirofumi メールアドレス: 所属:
URL	https://doi.org/10.24729/00008633

On the Fiber Texture Change during Drawing of initial $\{112\} \langle 111 \rangle$ and Goss Orientations in Aluminum Rod

Naotsugu INAKAZU*, Hisashi YAMAMOTO* and Hirofumi INOUE*

(Received November 15, 1980)

The mechanism was discussed of the development of fiber texture for the intermediate region of rod core, which was initially consisted of $\{112\} \langle 111 \rangle$ and Goss orientations. The discussion consists of two attempts to explain experimental orientation change from the initial orientations to $\{112\} \langle 111 \rangle$ and $\{110\} \langle 111 \rangle$ during drawing. The attempts are recorded of the biaxial and triaxial stress assumptions.

1. Introduction

In numerous papers, the mechanism of texture formation during rolling has been discussed, but there have been only a little papers on the development of fiber texture by drawing.

In our previous work¹⁾ on the correlation between fiber texture and torsion fatigue strength, we found that the texture of aluminum wire drawn up to 70% or 80% reduction in area consisted of $\{112\} \langle 111 \rangle$ and $\{110\} \langle 111 \rangle$ components, which hardly changed during torsion fatigue test. Thus we knew that these two components play an important role for the mechanical property of the drawn wire. Since it is of very interest to know the mechanism which leads to the formation of the two-component texture mentioned above, the orientation changes of the fiber texture during drawing aluminum wire were studied in this paper by X-ray pole figures. The changes were then analysed by lattice rotations due to active slip systems under biaxial and triaxial stress conditions.

2. Experimental Methods

Aluminum rod used for drawing was those produced industrially by "Properzi Method" which consists of continuous casting, followed by hot-rolling and full-annealing. The rod contains 0.10% Fe, 0.05% Si, 0.01% Cu, 0.004% Zn and 0.003% Cr, as impurities. The rod showed mainly Goss orientation in the peripheral region, $\{112\} \langle 111 \rangle$ orientation in the central region and both of them in the intermediate region.

The aluminum rod was drawn up to 93% reduction in area through usual conical dies with a half angle of 8° , with 15% reduction per each pass and at a rate of 20 m/min.²⁾ To prepare specimens for X-ray pole figures, thin plates were cut out of the intermediate region of the drawn wire and were thinned by electropolishing so that the final size of the plates should be 3 mm long in the axial direction of wire, 1 mm wide in the circumferential direction and 0.04 mm thick in the radial direction. Figure 1 illustrates the sectioning procedure.

* Department of Metallurgical Engineering, College of Engineering

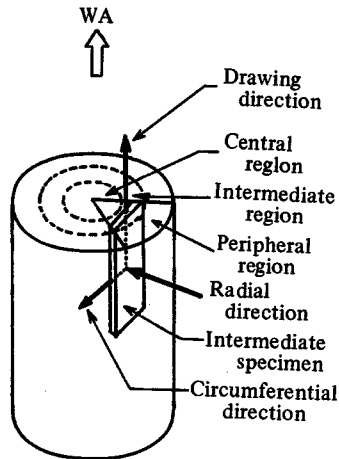


Fig. 1 Sectioning procedure.

The pole figures of the rod as well as drawn wires were made by using $\{111\}$ reflections of micro-beam $\text{CuK}\alpha$ radiation.

3. Experimental Results

The change of orientation during drawing was examined for wires drawn to 51, 72 and 93% reductions in area.

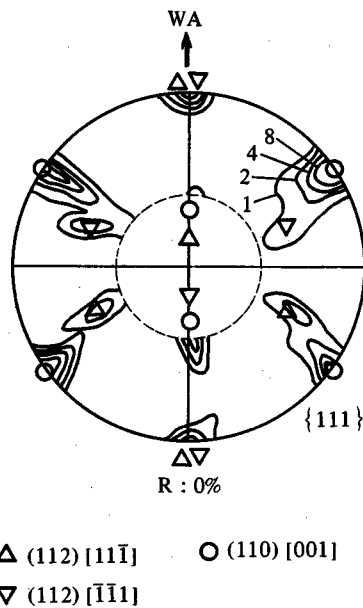
Fig. 2 $\{111\}$ pole figure at the intermediate region of aluminum rod material.

Figure 2 shows an $\{111\}$ pole figure of the initial fiber texture of the undrawn aluminum rod. It was found that the initial orientations consisted of $\{112\} \langle 111 \rangle$ and $\{110\} \langle 001 \rangle$ components, and there is only a little spread of intensity around the wire axis. Figure 3

shows a pole figure of the fiber texture at the intermediate region of the wire specimen drawn to 51% reduction in area. It was observed that the spread of $\{112\} \langle 111 \rangle$ component toward $\{110\} \langle 111 \rangle$ orientation and the rotation around the circumferential axis were occurring at 51% reduction.

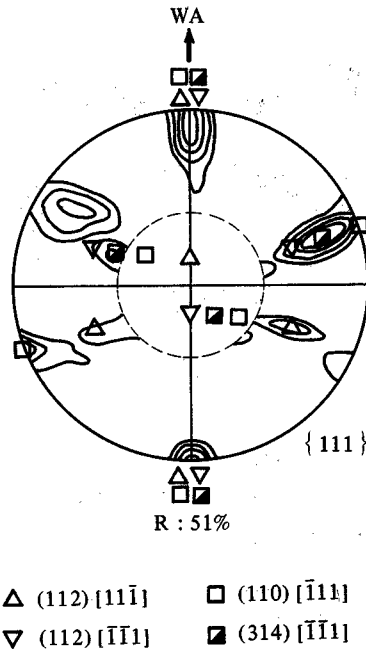


Fig. 3 $\{111\}$ pole figure at the intermediate region of the wire specimen drawn to 51% reduction in area.

Figure 4 shows an $\{111\}$ pole figure for the specimen drawn to 72% reduction. The orientation $(314) [\bar{1}\bar{1}1]$ and a new major orientation $\{110\} \langle 111 \rangle$ were developed and the $\{112\} \langle 111 \rangle$ orientation still remained to some extent.

During drawing up to 93% reduction, the $\{110\} \langle 111 \rangle$ component remarkably increased in X-ray intensity and the $\{112\} \langle 111 \rangle$ orientation was held in the spread of $\{110\} \langle 111 \rangle$. In the spread, the compressive plane was distributed continuously from $\{110\}$ to $\{112\}$ around the wire axis $\langle 111 \rangle$. The $\langle 100 \rangle$ fiber texture which existed in the undrawn rod throughly disappeared and then the single $\langle 111 \rangle$ fiber texture was developed to some extent as shown in Fig. 5. As mentioned above, two major components, $\{112\} \langle 111 \rangle$ and Goss orientation of undrawn rod changed into stable orientations, $\{110\} \langle 111 \rangle$ and $\{112\} \langle 111 \rangle$, with the orientation spread.

4. Discussion

To find the mechanism for the change of fiber texture mentioned above, we attempted two analyses by using slip systems that should be operative under two stress systems, i.e. biaxial and triaxial systems.

For the biaxial stress system, which Dillamore and Roberts³⁾ have proposed, a tensile

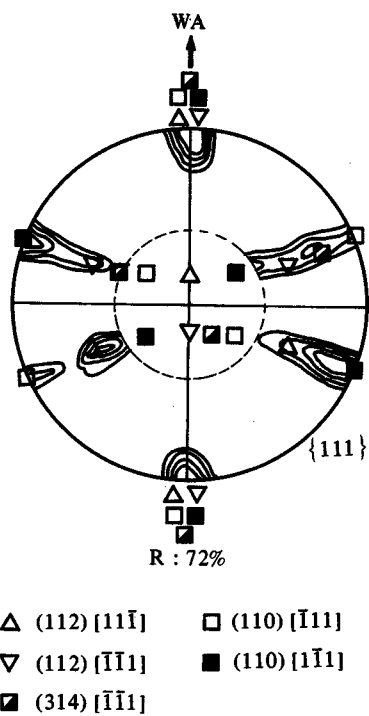


Fig. 4 $\{111\}$ pole figure at the intermediate region of the wire specimen drawn to 72% reduction in area.

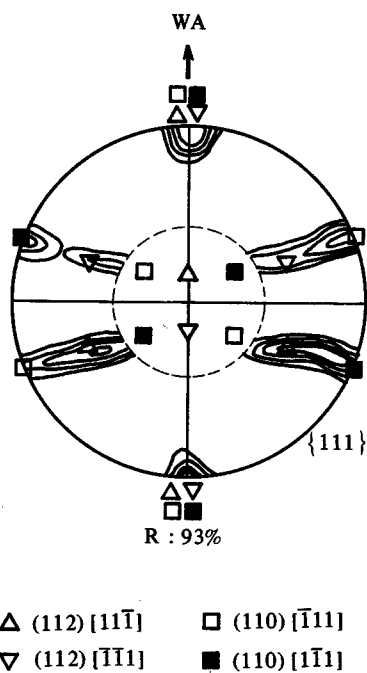


Fig. 5 $\{111\}$ pole figure at the intermediate region of the wire specimen drawn to 93% reduction in area.

stress (σ) parallel to the drawing direction and a compressive stress ($-\sigma$) perpendicular to the wire axis are taken to be the operative forces in drawing. The resolved shear stress of a slip system is given by

$$\tau = \sigma (\cos \phi_1 \cos \lambda_1 - \cos \phi_2 \cos \lambda_2) \tag{1}$$

where, ϕ_1 and λ_1 are angles made by the slip plane normal and the slip direction with the tensile axis, respectively, and ϕ_2 and λ_2 are angles made by the same slip elements with the compressive axis. Figure 6 shows the values of the relative resolved shear stresses of twelve $\{111\} \langle 110 \rangle$ slip systems in a range of orientation between $(110) [001]$ and $(112) [\bar{1}\bar{1}1]$.

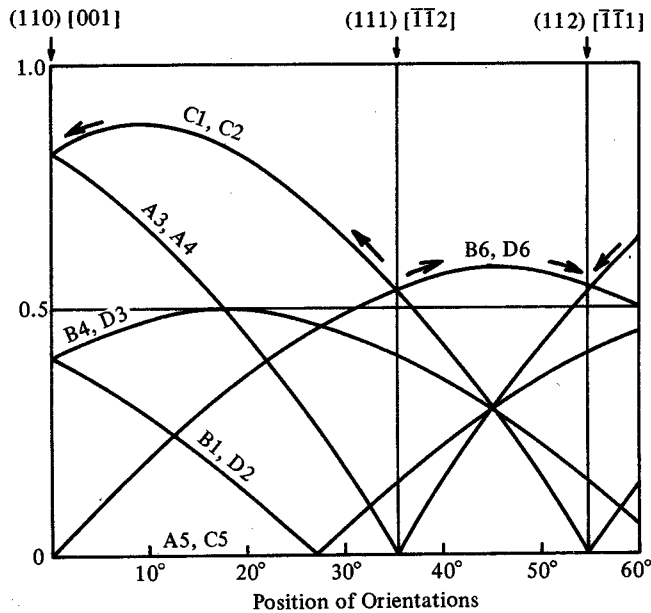


Fig. 6 Relative resolved shear stress of the twelve slip systems under the condition of the binary axial stress for the wire and compressive axes on the path $(110) [001] - (112) [\bar{1}\bar{1}1]$.

Slip plane normals A - D and slip directions 1 - 6 are shown in Fig. 7.

Near the $(110) [001]$ orientation, C 1, C 2 and A 3, A 4 slip systems possess high τ/σ values. And, even if the wire axis shifts toward the $(111) [\bar{1}\bar{1}2]$ orientation, the wire axis will be pushed back to $(110) [001]$ orientation by C 1, C 2 slip systems as shown by arrow marks in Fig. 6. Thus the $(110) [001]$ orientation is stable.

Near the $(112) [\bar{1}\bar{1}1]$ orientation, A 3, A 4 and B 6, D 6 slip systems possess high τ/σ values and operation of these slip systems will result no change in orientation, so $(112) [\bar{1}\bar{1}1]$ is also stable.

As a result of above analysis, we found that the biaxial stress assumption does not provide good explanation of the experimental results, since slip rotation actually initiated from the $(110) [001]$ and $(112) [\bar{1}\bar{1}1]$ orientations.

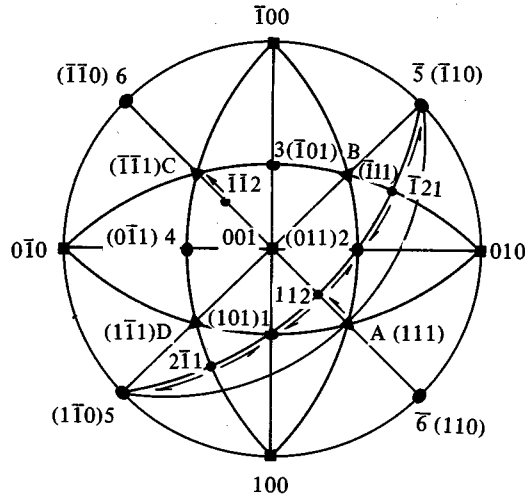


Fig. 7 Standard (001) stereographic projection illustrating the rotation of fiber texture.

In the triaxial stress system, a circumferential stress σ_3 is considered in addition to two stresses considered in the biaxial case, as shown in Fig. 8. Then the resolved shear stress is given by

$$\tau = \sigma_1 \cos \phi_1 \cos \lambda_1 + \sigma_2 \cos \phi_2 \cos \lambda_2 + \sigma_3 \cos \phi_3 \cos \lambda_3 \quad (2)$$

where, $\phi_1, \lambda_1, \phi_2$ and λ_2 are the same as those in biaxial stress system, ϕ_3 and λ_3 are angles made by slip plane normal and slip direction with the circumferential axis, respectively. Shear strains which correspond to σ_1, σ_2 and σ_3 are denoted by ϵ_1, ϵ_2 and ϵ_3 , respectively.

Assuming that ϵ_2 is equal to ϵ_3 because the hatched areas A and A' are similar, and observing the volume-constancy equation, $\epsilon_1 + \epsilon_2 + \epsilon_3 = 0$, one has

$$\epsilon_2 = \epsilon_3 = -\frac{1}{2} \epsilon_1 \quad (3)$$

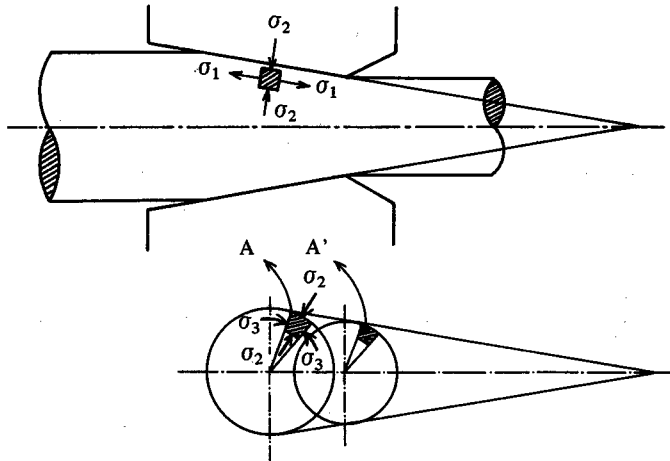


Fig. 8 Geometrical model of a drawing deformation under the trinary axial stress.

In the case of plastic deformation, the relation between stress and strain are obtained by the following equations,

$$\left. \begin{aligned} D \epsilon_1 &= \sigma_1 - \frac{\sigma_2 + \sigma_3}{2} \\ D \epsilon_2 &= \sigma_2 - \frac{\sigma_3 + \sigma_1}{2} \\ D \epsilon_3 &= \sigma_3 - \frac{\sigma_1 + \sigma_2}{2} \end{aligned} \right\} \quad (4)$$

where, D is a proportional constant, which corresponds to the Young's modulus (E). Substituting Eq. (3) into Eq. (4), one has

$$\sigma_2 = \sigma_3 = \sigma_1 - D \epsilon_1 \quad (5)$$

and the relation between cosines is given as follows,

$$\cos \phi_1 \cos \lambda_1 + \cos \phi_2 \cos \lambda_2 + \cos \phi_3 \cos \lambda_3 = 0 \quad (6)$$

From Eq. (5) and Eq. (6)

$$\tau = (\sigma_1 - \sigma_2) \cos \phi_1 \cos \lambda_1 \quad (7)$$

and assuming that

$$\begin{aligned} \sigma_1 - \sigma_2 &= D \epsilon_1 = \sigma' \\ \sigma' &= \sigma_1 + |\sigma_2| \end{aligned} \quad (8)$$

From the consideration of the volume of stress, σ' is the sum of two stresses, that is, $\sigma' = 2\sigma$ therefore

$$\tau = 2\sigma \cos \phi_1 \cos \lambda_1$$

Consequently, the relative resolved shear stress (τ/σ) are obtained from Eq. (9).

During drawing deformation the lattice rotations are on the assumption that the rotations occur around the perpendicular axis to a drawing and a compressive directions, and around the wire axis.

Figure 9 shows the relative resolved shear stress of $\{111\} \langle 110 \rangle$ slip systems over a range of orientations between (110) [001] and (112) $[\bar{1}\bar{1}1]$. It is considered that firstly the $\{110\} \langle 001 \rangle$ orientation changed into $\{112\} \langle 111 \rangle$ orientation through the $\{111\} \langle 112 \rangle$ orientation by rotation around the axis which is perpendicular to both the drawing and compressive directions, further, the above orientation changed into $\{110\} \langle 111 \rangle$ orientation by rotation around the wire axis $\langle 111 \rangle$. As shown in Fig. 9, near the (110) [001] orientation, B 4, D 3 and C 1, C 2 slip systems possess high τ/σ values, and when the wire axis shifts toward the (111) $[\bar{1}\bar{1}2]$ orientation the activities of C 1, C 2 slip systems decrease, while B 4, D 3 slip systems are still active due to their high τ/σ values. The operation of B 4, D 3 results in the change of the initial orientation into (111) $[\bar{1}\bar{1}2]$ orientation.

Near the (111) $[\bar{1}\bar{1}2]$ B 6, D 6 slip systems become active, instead of B 4, D 3 slip systems, consequently the migration of the orientation occurs toward the (112) $[\bar{1}\bar{1}1]$

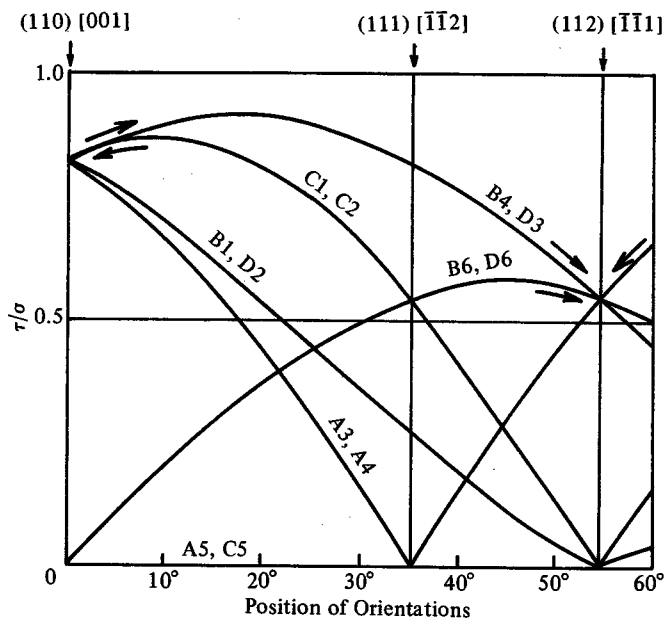


Fig. 9 Relative resolved shear stress of the twelve slip systems under the condition of the trinary axial stress for the wire and both compressive axes from (110) [001] to (112) $[\bar{1}\bar{1}1]$.

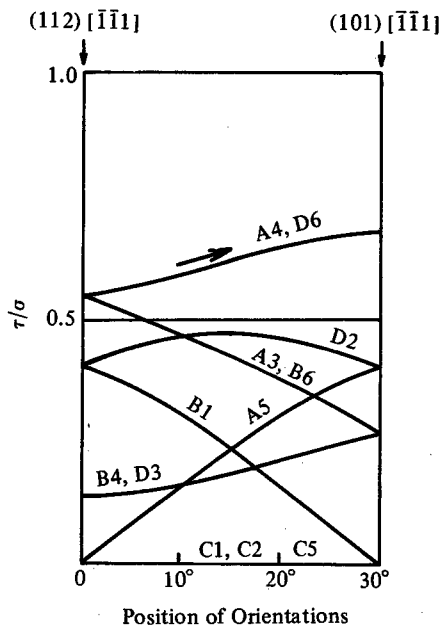


Fig. 10 Relative resolved shear stress of the twelve slip systems around the $[\bar{1}\bar{1}1]$ wire axis from (112) $[\bar{1}\bar{1}1]$ to (101) $[\bar{1}\bar{1}1]$.

orientation, and there is a little spread of intensity around the axis perpendicular to the drawing and compressive directions.

The above rotation is in good agreement with the experimental results in Fig. 3, 4 and 5. Figure 10 shows the values of relative resolved shear stress for a range of orientations

between $(112) [\bar{1}\bar{1}1]$ and $(101) [\bar{1}\bar{1}1]$. As shown in Fig. 10, A 4 and D 6 slip systems exist the highest τ/σ values between $(112) [\bar{1}\bar{1}1]$ and $(101) [\bar{1}\bar{1}1]$ orientation, and then the compressive plane is inclined to be parallel to the A(111) and D($\bar{1}\bar{1}1$) planes, consequently by the interaction of $(111) + (\bar{1}\bar{1}1) \rightarrow (101)$ the plane rotation around the $\langle 111\rangle$ wire axis occurs and the $(101) [\bar{1}\bar{1}1]$ orientation is developed, but there is a little spread of intensity around the wire axis as shown in Fig. 5. Furthermore, also from Calnan's proposal⁴⁾ the development of the $\{110\}\langle 111\rangle$ orientation is explained as shown in Fig. 7. It is considered that the compressive plane normal to a radial direction of the wire is accompanied with the $\{110\}$ plane, therefore the rotation around the $\langle 111\rangle$ axis occurs and the $\{110\}\langle 111\rangle$ component is developed.

5. Conclusions

In order to find the process which leads to fiber texture formation at the intermediate region in a aluminum wire rod, the slip rotations corresponding to the changes of orientation were studied.

The results were as follows:

The slip rotations in actual texture changes were not well explained by slip systems which should be operative under the biaxial stress system, but well explained if the triaxial stress system was considered.

The change of the initial Goss orientation of undrawn wire rod into $\{112\}\langle 111\rangle$ orientation was explained to occur by rotation around the axis which is perpendicular to the drawing and compressive directions owing to the operation of $\{111\}\langle 110\rangle$ slip systems, which have the maximum values of relative resolved shear stress. Further, the rotation around the wire axis resulted in the rotation of the above orientation into $\{110\}\langle 111\rangle$ orientation and the occurrence of the spread between $\{112\}\langle 111\rangle$ and $\{110\}\langle 111\rangle$ orientations. The occurrence of the spread is attributed to a slight difference between values of relative resolved shear stresses for $\{110\}\langle 111\rangle$ and $\{112\}\langle 111\rangle$ orientations.

Acknowledgment

The authors would like to acknowledge the financial support of the Light Metal Educational Foundation, Incorporated, Osaka, Japan.

References

- 1) N. Inakazu and H. Yamamoto, *Trans. Japan Inst. Metals*, 18 265 (1977).
- 2) H. Yamamoto and N. Inakazu, *J. Japan Soc. Tech. Plasticity*, 12 284 (1971).
- 3) I.L. Dillamore and W.T. Roberts, *Acta Met.* 12 281 (1964).
- 4) E.A. Calnan, *Acta Met.* 2 865 (1954).